INSTITUT DE PHYSIQUE DE L'UNIVERSITE DE NEUCHATEL

DESORDRE SUPERFICIEL DE LA GLACE MONOCRISTALLINE ETUDIE ENTRE -191°C ET -2°C PAR CANALISATION DE PROTONS DE 100 KEV

Thèse présentée à la Faculté des Sciences
de l'Université de Neuchâtel
pour l'obtention du grade de Docteur ès Sciences

par

Ilan GOLECKI

M.Sc. (Physics)

B.Sc. Cum Laude (Physics)

Janvier 1978

IMPRIMATUR POUR LA THÈSE

Désordre superficiel de la glace monocristalline étudiée entre -191°C et -2°C par canalisation de protons de 100 keV

de Monsieur Ilan Golecki

UNIVERSITÉ DE NEUCHATEL

FACULTÉ DES SCIENCES

La Faculté des sciences de l'Université de Neuchâtel, sur le rapport des membres du jury,

Messieurs C. Jaccard, J. Rossel, A. Aegerter et J.H. Bilgram (EPF Zurich)

autorise l'impression de la présente thèse sans exprimer d'opinion sur les propositions qui y sont contenues.

Neuchâtel, le 15 mars 1978

Le doyen : J.-P. Schaer

J.-P. Schaer

THE SURFACE OF ICE NEAR 0°C STUDIED BY 100 keV PROTON CHANNELING

I. GOLECKI and C. JACCARD
Institut de Physique de l'Université, Rue A.-L. Breguet 1, CH-2000 Neuchâtel, Switzerland

Received 27 June 1977

The basal plane of ice in thermodynamic equilibrium with the vapor is studied by means of 100 keV proton channeling between −130°C and −2°C. The minimum yield increase rapidly above-35°C, indicating the existence of a 90 nm thick disordered layer at −2°C.

The properties of the surface of ice have attracted scientific interest for more than a century. Various indirect measurements have indicated the existence of a disordered, "liquid-like" layer at the ice surface in equilibrium between −35°C and 0°C. These include mechanical [1], electrical [2], molecular diffusion [3], gas adsorption [4], and especially NMR [5] studies, and more recently photoemission [6] and Volta effect [7] measurements. Experimental estimates of the thickness of this layer range from 2 nm to 100 nm at −1°C, while a structural model proposed by Fletcher [8] tends towards the lower limit. However, the presence of this layer has not yet been detected by direct experimental methods. One such suitaole method is the channeling technique [9] of nuclear backscattering, which has been applied in the past to the study of lattice defects in single crystals. In particular the use of 100 keV protons as opposed to more energetic or heavier particles results in the best depth resolution obtainable in ice [10]. In addition, the stopping power in the aligned and random directions is the same [11], and the RBS cross-section is higher at 100 keV.

Because of the need to keep the ice crystal in thermodynamic equilibrium with its own vapor (e.g. 4.2 torr at −1°C) during the measurement, a conventional, high-vacuum scattering chamber cannot be used. Therefore a special apparatus has been developed, in which the proton beam is injected into a windowless scattering chamber through a fine, 3° conical nozzle, having an end aperture 0.1 mm in diameter. The nozzle can be brought up to the surface of the crystal even in the case of grazing incidence [12], thus minimizing the path of the beam in the water vapor. In this way, the initial 0.05° collimation of the beam is not degraded by the vapor, enabling channeling studies to be carried out normally. The various effects of the vapor on the experimental results have been analyzed in extensive test runs, and are either completely negligible, or can be taken into account in the evaluation of the data. Further details on the construction and performance of the apparatus are included in a separate publication [13].

In the work reported here, 100 keV proton energy spectra backscattered at 150° from the basal plane of ice were measured along, and 10° off the *c*-axis (aligned and random directions, respectively), between −130°C and −2°C. The beam was incident normally on the ice surface with a typical flux of 5×10^{12} $H^+/cm^2 \cdot s$, care being taken to avoid radiation damage at the lower temperatures [14] by distributing the dose on the crystal surface. The nozzle-crystal distance was 1 mm. The pure ice crystals were cut from a larger oriented crystal (kindly provided by Dr. J.H. Bilgram, ETH, Zürich), and mounted on the tip of a gas exchange cryostat [15]. The cryostat was part of a goniometric assembly having four degrees of freedom for rotation, tilt, horizontal and vertical translation [13, 15]. The backscattered protons were detected by means of a 25 mm^2 Si surface-barrier detector (Ortec Premium), kept at a slightly higher temperature than the surrounding vapor in order to avoid condensation. The overall energy resolution was 5.3 keV in vacuum (6.1 keV at 4.2 torr H_2O), corresponding to a depth resolution in ice of 29 nm (33 nm). The crystal temperature and H_2O pressure were measured with a calibrated Cu-constantan thermocouple and capacitance manometer (model 220 MKS Baratron), respectively.

The temperature dependence of the minimum yield χ as a function of depth z is illustrated in fig. 1, while that of the extrapolated surface minimum yield χ_0 is

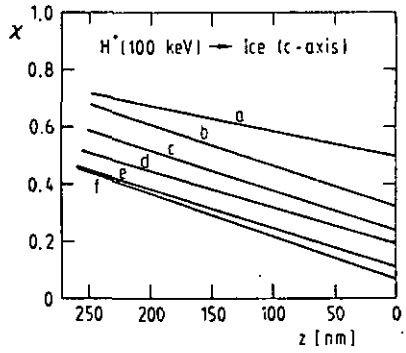

Fig. 1. Dechanneled fraction χ versus depth z for 100 keV protons in ice (c-axis) at the following temperatures: (a) −1.8°C, (b) −6°C, (c) −13°C, (d) −20°C, (e) −35°C, and (f) −55°C. A stopping power of 84.6 ± 8 eV/nm taken from Whaling [10] was used to determine the depth scale.

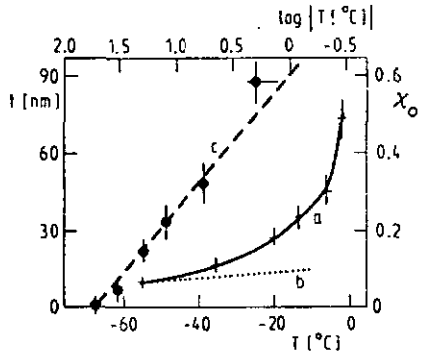

Fig. 2. Extrapolated surface minimum yield χ_0 in ice (c-axis) versus T (°C): (a) as measured, and (b) as calculated from Barrett's formula [16], using the thermal vibration amplitudes given in [17]. The dashed line (c) shows the thickness, t, of the disordered surface layer, assumed amorphous, versus $\log|T(°C)|$, as calculated with the aid of Meyer's theory [18] (see text).

given in fig. 2. Below −60°C the small increase of χ with T is due only to the influence of thermal vibrations of the O and H atoms perpendicular to the c-axis (although the H atoms do not contribute to backscattering). However, for $T > -35$°C the remarkable increase of χ is much larger than expected from harmonic vibrations alone, even when using Barrett's formula [16], which gives for ice at low temperatures values of χ_0 and $d\chi_0/dT$ larger than measured. The dechanneling length $z_{1/2}$ is only slightly reduced between −55°C and −2°C. These results, which could be reproduced upon thermal cycling, indicate the formation of a (partially) disordered layer at the crystal surface. In order to estimate the thickness of this layer, one may use Meyer's theory of multiple scattering [18] as explained by Campisano et al. [19] and summarized in the following equation

$$\chi(z) = P + \chi_s(z)\,[1 - P]\ ,$$

where $\chi(z)$ and $\chi_s(z)$ are the dechanneled fractions with and without the disordered layer, respectively, and $P = P[\psi_{1/2}(z), \tau]$ is Meyer's integral distribution for an amorphous layer of reduced thickness τ. When applying this equation to the present case, $\chi(z)$ is the measured minimum yield at temperature T, $\chi_s(z)$ is the extrapolated yield at T due only to harmonic vibrations, and $\psi_{1/2}$ is the extrapolated half-angle at T. The extrapolations were done by using χ_s and $\psi_{1/2}$ values measured at low temperature, together with $d\chi_s(0)/dT = 6 \times 10^{-4}$/K and Barrett's formula for $\psi_{1/2}$ [16]; values of $P(\theta, \tau)$ were taken from Lugujjo and Mayer [20]. The thickness, t (nm), of the equivalent amorphous layer obtained by this procedure is seen in fig. 2 to increase approximately as $-50 \cdot \log|T(°C)|$, which is the empirical functional dependence predicted by Fletcher [8], but with a twenty-fold larger slope. The value of $t = 90$ nm at −1.8°C agrees, however, with estimates from mechanical measurements [1] and with Weyl's suggestion [21]. Since neither $\log(\chi - \chi_s)$ nor $\log t$ depend linearly on $\log|T(°C)|$, no critical exponent can be assigned. The large increase of χ near the melting point in ice may be due to anharmonic (surface) vibrations or soft modes. In fact, Pavalow and Zajac [17] have observed an anomalously large increase in the H thermal vibration amplitude in ice parallel to the c-axis between −10°C and −0.5°C. The absence of similar measurements for thermal vibrations perpendicular to the c-axis near 0°C prevents a direct comparison with the present results.

In conclusion, the present channeling study reveals by the first direct measurement the existence of a disordered surface layer in ice above −35°C. The thickness of this layer is 90 nm at −1.8°C, which is 20 times larger than the value predicted by Fletcher's theory [8]. Additional work on this project is in progress.

This work was supported by the Swiss National Science Foundation. It forms part of the Thesis to be submitted by I. Golecki to the Faculty of Sciences,

University of Neuchâtel, in partial fulfilment of the requirements for the degree of Ph.D. in Physics.

References

[1] H.H.G. Jellinek, Water and aqueous solutions (Wiley, New York, 1972) ch. 3;
S.C. Colbeck, to be published in: Proc. Symp. Physics and chemistry of ice (Cambridge, 1977) in J. Glaciol.

[2] C. Jaccard, Physics of snow and ice, vol. 1 (Hokkaido University, Sapporo, 1967) 173;
N. Maeno and H. Nishimura, to be published in: Proc. Symp. Physics and chemistry of ice (Cambridge, 1977) in J. Glaciol.

[3] W.D. Kingery, J. Appl. Phys. 31 (1960) 833.

[4] M.W. Orem and A.W. Adamson, J. Colloid Interface Sci. 31 (1969) 278.

[5] V.I. Kvlividze, V.F. Kiselev, A.B. Kurzaev and L.A. Ushakova, Surf. Sci. 44 (1974) 60.

[6] D. Nason and N.H. Fletcher, J. Chem. Phys. 62 (1975) 4444.

[7] E. Mazzega, U. del Pennino, A. Loria and S. Mantovani, J. Chem. Phys. 64 (1976) 1028.

[8] N.H. Fletcher, in: Physics and chemistry of ice (Royal Society of Canada, Ottawa, 1973) p. 132.

[9] D.S. Gemmel, Rev. Mod. Phys. 46 (1974) 129.

[10] W. Whaling, in: Handbuch der Physik, vol. XXXIV (Springer, Berlin, 1958) p. 193.

[11] G. Della Mea et al., Atomic collisions in solids (Plenum Press, New York, 1975) p. 75.

[12] J.S. Williams, Nucl. Instr. Meth. 126 (1975) 205.

[13] I. Golecki and C. Jaccard, to be published in: Proc. 3rd Int. Conf. Ion beam analysis (Washington, D.C., 1977) in Nucl. Instr. Meth.

[14] I. Golecki and C. Jaccard, to be published in: Proc. Symp. Physics and chemistry of ice (Cambridge, 1977) in J. Glaciol.

[15] H. Huber, Thesis (University of Neuchâtel, Switzerland, 1974).

[16] J.H. Barrett, Phys. Rev. B3 (1971) 1527.

[17] M. Pavalow and A. Zajac, in: Physics and chemistry of ice (Royal Society of Canada, Ottawa, 1973) p. 128.

[18] L. Meyer, Phys. Stat. Solidi (b) 44 (1971) 253.

[19] S.U. Campisano, G. Foti, F. Grasso and E. Rimini, Phys. Rev. B8 (1973) 1811.

[20] E. Lugujjo and J.W. Mayer, Phys. Rev. B7 (1973) 1782.

[21] W.A. Weyl, J. Colloid Sci. 6 (1951) 389.

NUCLEAR INSTRUMENTS AND METHODS 149 (1978) 689-694 ; © NORTH-HOLLAND PUBLISHING CO.

AN APPARATUS FOR CHANNELING EXPERIMENTS AT TORR PRESSURES

I. GOLECKI and C. JACCARD

Institut de Physique de l'Université, Rue A.-L. Breguet 1, CH — 2000 Neuchâtel, Switzerland

A novel system is described which enables channeling experiments with 100 keV protons to be carried out at an ambient pressure of a few torr. The system was constructed in order to study the surface of ice in equilibrium with its own vapor near its melting point. The principal advantages of 100 keV vs MeV protons are maximum depth resolution, equal stopping power in the aligned and random directions, and a higher RBS cross-section. The proton beam enters the windowless scattering chamber through a 3° conical nozzle, having a 0.1 mm diameter end aperture. The nozzle can be moved along the beam axis, so as to bring it as close as possible to the crystal surface, even in the case of grazing incidence. The size of the aperture is determined as a compromise between the requirements of small beam divergence and low vapor consumption on the one hand, and small edge scattering effects and sufficient beam current on target, on the other. Test runs performed at 4 torr H_2O showed no measurable influence on the channeling yield of a LiF crystal, with the nozzle 1 mm away from the crystal surface. The energy loss due to vapor in the nozzle was only 1.5 keV, equivalent to 1.7 torr·cm. The nozzle throughput at 4 torr was 7.2 mg H_2O/h, enabling extended measurements with a relatively small sample to be carried out.

1. Introduction

Channeling is one of the important techniques for studying lattice disorder in single crystals[1]). Such studies have up to the present been done in high or ultra-high vacuum. However, in certain situations the target has to be kept in a controlled, non-vacuum atmosphere during the measurement. A case in point is provided by ice in thermodynamic equilibrium near its melting point, where e.g. at −1 °C its vapor pressure is 4.2 torr. The interest in ice has arisen because of a large number of indirect measurements[2]) which have indicated the existence of a disordered, "liquid-like" layer at the ice surface near its melting point. Estimates of the thickness of this layer range from 2 nm to 100 nm at −1 °C, but as yet its presence has not been detected by direct experimental methods. Therefore, it was decided to develop a system which would enable channeling measurements with our 100 keV proton accelerator to be carried out while keeping the ice target in equilibrium with its own vapor. The principal advantages of 100 keV vs higher energy protons are threefold: (1) maximum depth resolution, which corresponds to the maximum in the stopping power curve, occurs around 100 keV[3]); (2) the stopping power, and therefore the depth scale in the aligned and random directions are roughly equal at low energies[4]), thus simplifying data analysis; (3) the RBS cross-section is much higher at low energies.

The apparatus which has been developed is based on a windowless scattering chamber, into which the proton beam is injected through a narrow nozzle. Extensive test runs have demonstrated the ability to carry out channeling experiments at an ambient pressure of a few torr with no measurable influence of the vapor on the channeling yield. The construction and performance of the system are described in the following sections.

2. Description of the apparatus

2.1. Introduction

A cutaway view of the system is given in fig. 1. The high pressure chamber (HPC) is fixed inside a larger scattering chamber (LSC), which has been described elsewhere[5,6]) in connection with channeling studies in high vacuum. The 200 mm diameter LSC is evacuated by means of a 350 l/s turbomolecular pump (Leybold–Heraeus) to a hydrocarbon-free vacuum of 1×10^{-6} torr. A differential pumping system allows the introduction of gaseous targets in the LSC up to 0.1 torr without affecting the pressure in the accelerator. The top flange of the LSC accomodates a goniometer, shown in fig. 2, on which can be mounted one of several variable-temperature crystal holders. The goniometer has four degrees of freedom: rotation ϕ (360°/precision 0.05°), tilt ψ (±10°/0.025°), vertical and horizontal translation (20 mm/0.01 mm and 12 mm/0.005 mm, respectively). Leak-tightness with respect to the atmosphere is assured by means of a circumferential O-ring during rotation. The other three degrees of freedom utilize the elasticity of a stainless steel bellows.

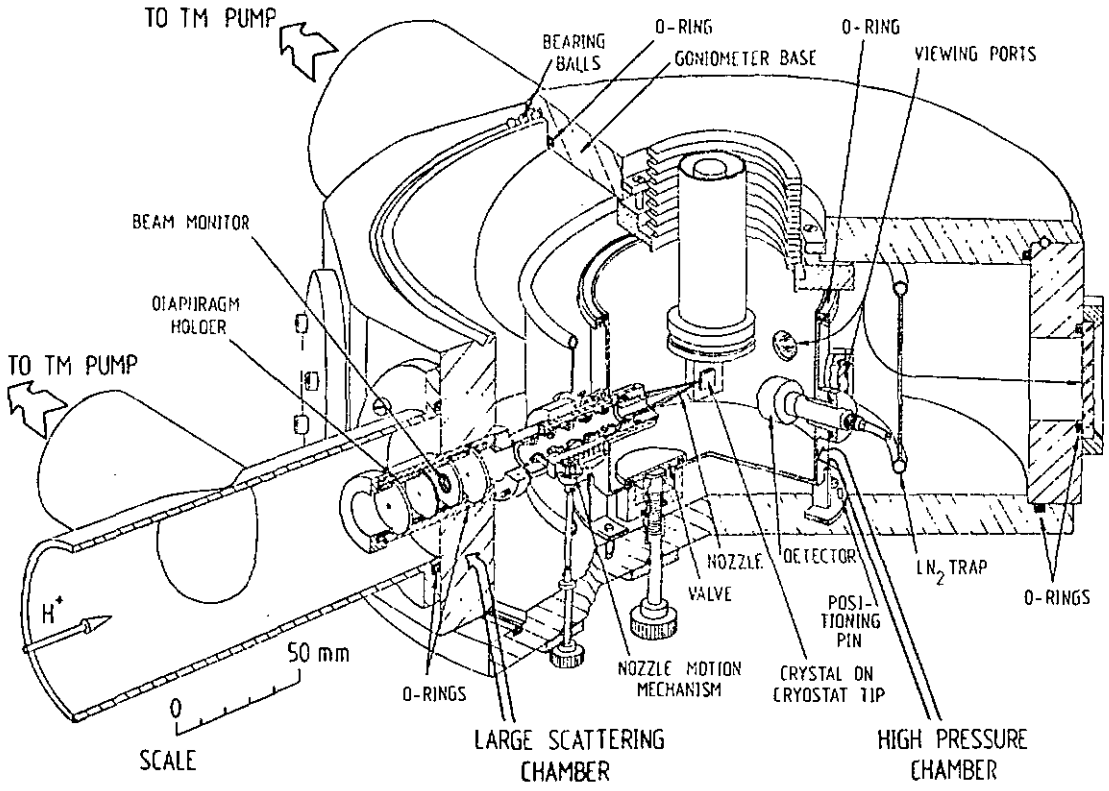

Fig. 1. A simplified pictorial view of the high-pressure channeling apparatus.

The 100 keV, 1 mm diameter proton beam is collimated by the ion optics to 0.05°. The beam intensity is measured by intercepting part of it on a Micromesh nickel grid (EMI Electronics Ltd.) of cell size $125 \times 125\ \mu m^2$ and 75% transmission. The grid, which is biased to +45 V in order to suppress the emission of secondary electrons, is part of a diaphragm assembly which determines the beam direction and its diameter. A model 602 Keithley electrometer is connected to the grid and used to control data acquisition. The scattered protons are detected by means of a Si surface-barrier detector (Ortec Premium) connected to standard spectroscopy electronics. The energy resolution obtained with a 25 mm^2 detector operated at room temperature is 5.3 keV, corresponding to a depth resolution in ice of 29 nm for 150° backscattering.

2.2. Initial design considerations

The principal requirement of apparatus was that it enable channeling measurements to be carried out at an ambient pressure of up to 4.6 torr (i.e. the vapor pressure of ice at 0 °C). Since an initially collimated beam of particles becomes divergent when passing through a dense medium, the ingoing path of the proton beam in the vapor had to

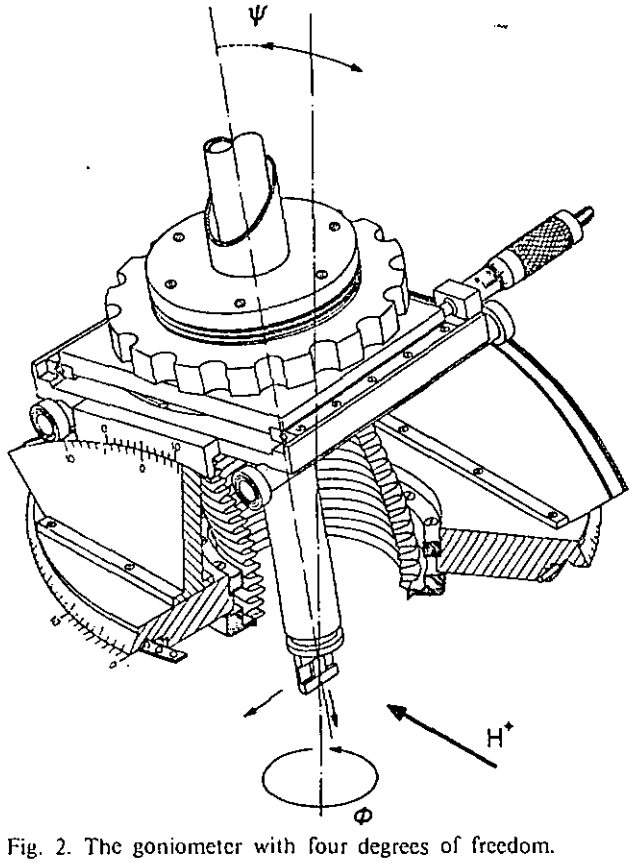

Fig. 2. The goniometer with four degrees of freedom.

be minimized. The full-angle beam divergence in H_2O vapor was calculated with the aid of Meyer's theory[7]) to be 0.015°/torr·mm. Thus the use of even the thinnest entrance window[8]) had to be ruled out, and a windowless design was decided upon. Other requirements were:

1) The possibility of measurement at grazing incidence, in order to improve the depth resolution[9]).

2) The ability to maintain high vacuum in the accelerator and to measure the incident charge by the method described in Sect. 2.1. The latter requirement implied a pressure smaller than 10^{-4} torr in the LSC [10]).

3) The ability to operate the detector normally and with optimum resolution.

4) The possibility of obtaining high vacuum in the vicinity of the ice crystal at low temperature.

5) Compatibility with the existing equipment and easy conversion between the two modes of operation. These considerations led to the construction of the HPC described below.

2.3. High pressure chamber

The stainless steel, 84 mm diameter HPC is fixed inside the LSC on three intermediate legs. The proton beam is brought in through a fine conical nozzle (3° or 6° half-angle), having an end aperture 0.1 mm in diameter. The nozzle can be moved along the beam axis from the outside. It can thus be brought up to the surface of the crystal even in the case of grazing incidence. Leak tightness between the HPC and the LSC is assured by means of an O-ring located in a groove on the top flange of the HPC, and pressing against a flat surface on the goniometer base. Thus all four degrees of freedom of the goniometer are kept. This construction necessitated careful design and close tolerances.

The size of the nozzle aperture was determined as a compromise among several conflicting requirements. A minimal opening was required in order to create an abrupt pressure gradient between the hp and the high vacuum regions, and to ensure low vapor consumption and thus a longer life for the ice crystal. On the other hand, a reasonably large aperture was needed in order to let enough beam current reach the target, and also to minimize possible edge-scattering effects. The choice of 0.1 mm diameter was found to fulfil these requirements rather well. Results of test measurements are presented in section 3. The nozzles were machined in aluminum by using drills having successively smaller diameters. The end aperture was pierced with a specially prepared tool over a depth smaller than its diameter, and subsequently polished with a 20 μm Cu–Be wire. The nozzle motion mechanism derives its alignment from the diaphragm holder (fig. 1). The nozzle itself fits tightly on a nozzle holder to which it is glued. The stainless steel nozzle holder is screwed onto a brass tube, the two having been mechanically adjusted for a snug fit. The tube has side openings to enable lateral pumping of the nozzle. This tube can slide inside another fixed brass tube, the latter being mounted on the diaphragm holder. The fixed tube also has clearances for lateral pumping. The movement of the nozzle, nozzle holder, and first brass tube is effected by means of a rack and pinion mechanism. A keyed shaft provides the coupling between the pinion and a rotary motion feedthrough on the base-plate of the LSC. The feedthrough is connected on the atmospheric side to a gear train (not shown in fig. 1) and handle. In this way the nozzle can be moved over a total distance of 23 mm with a precision better than 0.1 mm. The exact position can be read on a vernier. O-rings located in the wall of the HPC and in the nozzle holder provide the necessary leak tightness between the two scattering chambers. After the initial alignment, no further adjustments have been necessary in almost a year of operation. The alignment with respect to the beam could be reproduced along the entire course of nozzle motion, even after dismantling and reinstalling the whole mechanism and the HPC.

2.4. System performance

We next review the performance of the system as regards the other requirements outlined in Sect. 2.2. Charge integration is done as before, since even at the highest working pressure of 4.6 torr in the HPC, the pressure in the LSC is only 3×10^{-5} torr. This can be further reduced to 2×10^{-6} torr by cooling with LN_2 a 500 cm^2 copper trap installed in the LSC. The detector is operated inside the HPC and brought close to the crystal surface in order to minimize energy straggling and loss[11]). Condensation of water vapor on the detector is prevented by keeping it slightly warmer than the surrounding vapor. With this precaution no degradation in performance has been observed. Two valves (only one is shown in fig. 1) which

connect the HPC to the LSC, allow the former to be evacuated to 4×10^{-6} torr. In order to minimize mechanical stresses on the HPC and to enable its quick installation and dismantling, use is made of gear mechanisms (omitted for simplicity in fig. 1) to couple the valves to rotary motion feedthroughs. The positive charge carried by the proton beam is neutralized at the surface of the insulating target by means of secondary electrons conveniently emitted by the grounded nozzle itself. Tests carried out in vacuum have shown this neutralization to be highly effective. Additional electrons, which originate from ionization of the water vapor, as well as positive ions, naturally are present also. Other features of the HPC include a flexible connection to an ion gun, which is mounted at 120° on the LSC. Thus the gun can be used for surface sputtering (in vacuum) and heavy marker implantation. Viewing ports equipped with magnifying lenses enable careful positioning of the nozzle near the crystal surface. The volume filled with H_2O vapor is 1.2 l. The H_2O pressure is measured with a model 220 MKS Baratron capacitance manometer. This absolute gauge has a precision of 10^{-3} torr and a temperature coefficient of 10^{-3} torr/°C over its range of 10^{-3}–10 torr. A Balzers model IMR 110 hot-cathode ionization gauge is used in the high vacuum range.

3. Operational experience

The presence of water vapor affects the measured RBS spectra in the following major ways: (1) energy loss of the incoming and scattered beams, (2) energy straggling, (3) vapor peak, (4) beam divergence. All of these effects increase with pressure, and are thus minimized by bringing the nozzle as close as possible to the crystal surface. In practice, it was found that a nozzle-crystal distance of about 1 mm was a safe minimum for work with ice.

The energy loss and straggling were determined as a function of H_2O pressure and nozzle position by scattering off a 1 nm evaporated layer of Au on a Be substrate. Specifically the position and fwhm of the gold peak were measured and used together with the known geometry and stopping power[11]). The incoming beam suffers an energy loss inside the nozzle (9% of the total loss) and between the nozzle and the crystal surface (2.5%). However, by far the largest portion of energy loss (88.5%) occurs in the path of the scattered beam between the crystal surface and the detector. These values obtain when the nozzle is 1 mm away, and the 25 mm² detector 29 mm away from the crystal surface. Differences in path length resulting from the 11° acceptance angle of the detector are negligibly small. The energy loss in the nozzle is thus seen to be a relatively minor effect, e.g. at 4 torr it is equivalent to only 1.7 torr·cm of water vapor, decreasing proportionately at lower pressures. The small overall number of H_2O molecules in the nozzle is indicative of the abruptness of the pressure gradient that is usually associated with supersonic flow[12]). In additional tests with air up to 1 atm pressure no particular problems were encountered. However, the energy loss becomes prohibitively large above ≈20 torr. The energy straggling due to the vapor is added in quadrature to the resolution of the detector. The magnitude of the effect amounts to about 0.6 (keV)²/torr·cm (fwhm)² [13]), which causes an increase of ≈15% in the resolution for a worst case pressure of 4.6 torr in the above geometry. Scattering off the H_2O vapor present between the nozzle and the crystal surface gives rise to a vapor peak, which is superimposed on the RBS spectrum from the ice crystal. The effect is rather small, however, since 1 torr·mm of H_2O vapor is equivalent to 1.15 nm (or about 3 monolayers) of solid ice, and it can be taken into account in the data analysis. Note that the three effects outlined above influence the random and the aligned spectra in exactly the same way.

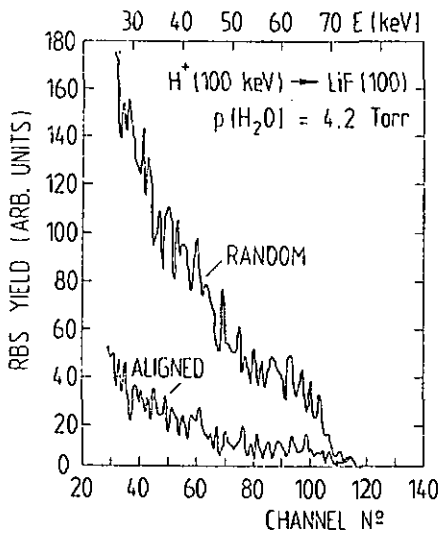

Fig. 3. Energy spectra of 100 keV protons backscattered at 150° from a LiF crystal, at an ambient pressure of 4.2 torr H_2O. Nozzle-crystal distance: 1 mm. Depth scale: 1.6 nm/channel.

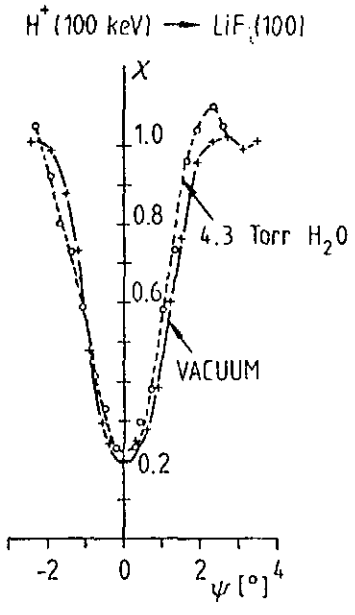

Fig. 4. Axial channeling dip of 100 keV protons backscattered at 150° from a LiF crystal in high vacuum and at 4.3 torr H_2O. Thickness of scattering zone is 50 nm beneath the surface. Nozzle–crystal distance: 1 mm.

In order to assess the importance of beam divergence, extensive test runs were performed with W and LiF crystals at room temperature. Fig. 3 shows aligned and random energy spectra for a LiF crystal, measured at an ambient pressure of 4.2 torr H_2O, with the nozzle 1 mm away from the crystal surface. Similar spectra measured in high vacuum (and omitted in fig. 3 for the sake of clarity) are merely displaced to higher energies, the surface minimum yield of 0.15 being the same within the statistical accuracy. An example of angular scans in high vacuum and in 4.3 torr H_2O is shown in fig. 4. The two channeling dips are seen to be practically the same, with respect to both the minimum yield and to the fwhm. Minor differences may be due to the fact that the two scans did not originate from exactly the same area on the crystal surface. Additional test runs with a W single crystal yielded similar results. Moreover, measurements of beam spot size as a function of pressure and nozzle position were performed, using Kodak CA-80-15 cellulose nitrate track detectors[14]). The results obtained substantiated the above channeling experiments, yielding in addition a value of $\approx 0.013°$/torr·mm for the full-angle beam divergence in H_2O vapor, in good agreement with Meyer's theory[7]). Thus it is seen that the main design goal of the apparatus, namely the possibility to carry out channeling studies under good conditions at torr · pressures has been achieved. The good collimation of the beam which emerges from the nozzle can be attributed to the small size of the end aperture and to the step-like interior structure of the nozzle. Comparison of RBS energy spectra measured in high vacuum with and without the nozzle showed the absence of edge scattering effects. The beam current which passes through the nozzle is quite sufficient for measurements on ice, typical current on target being 0.1 nA, while the maximum achievable current is about 1.5 nA. The measured throughput of the nozzle in the laminar regime increases linearly with pressure in the HPC, being e.g. equal to 7.2 mg H_2O/h at 4 torr. Extended runs with a relatively small ice sample can thus be carried out. No carbon buildup occurs during high pressure backscattering, due to the clean vacuum conditions of the scattering chambers and the accelerator.

Following the satisfactory results obtained in the various test runs, we proceeded with channeling measurements on ice single crystals, extending the previously accessible temperature range up to −1 °C. The most important result observed has been a rapid increase of minimum yield with temperature above about −35 °C, indicating the formation of a disordered phase. These results thus substantiate the hypothesis of a "quasi-liquid" region in ice near its melting point[2]). A more detailed account of these experiments will be published elsewhere.

4. Conclusions

The system which has been described enables channeling experiments to be carried out for the first time at ambient pressures of a few torr with a 100 keV proton beam. Measurements on ice single crystals have been extended from the LN_2 temperature range up to −1 °C. These show a remarkable increase of minimum yield with temperature above −35 °C, thus substantiating by direct measurement the existence of a disordered phase in ice near its melting point. Results of these experiments, which are still in progress, will be published elsewhere. The high pressure apparatus can also be used, with suitable modifications, in other cases where charged particle analysis is to be performed on a sample kept in a controlled atmosphere. A system of similar design should prove valuable for work with nonstoichiometric compounds, such as oxides in equilibrium with

CO_2/CO or H_2O/H_2 mixtures[15]), with liquid crystals and other volatile materials.

We wish to acknowledge the valuable technical assistance and exacting craftsmanship of J. P. Bourquin and J. S. Margot. This work was supported by the Swiss National Science Foundation. It forms part of the Thesis to be submitted by I. Golecki to the Faculty of Sciences, University of Neuchâtel, in partial fulfilment of the requirements for the degree of Ph. D. in Physics.

References

1) D. S. Gemmel, Rev. Mod. Phys. 46 (1974) 129.
2) H. H. G. Jellinek, *Water and aqueous solutions* (Wiley, New York, 1972) ch. 3; E. Mazzega, U. del Pennino, A. Loria and S. Mantovani, J. Chem. Phys. 64 (1976) 1028.
3) H. K. Reynolds, D. N. F. Dunbar, W. A. Wenzel and W. Whaling, Phys. Rev. 92 (1953) 742.
4) G. Della Mea, A. V. Drigo, S. Lo Russo, P. Mazzoldi and G. G. Bentini, *Atomic collisions in solids*, Gatlinburg, Tenn., 1973 (Plenum Press, New York, 1975) p. 75; F. F. Komarov and A. F. Burenkov, Rad. Eff. 29 (1976) 201.
5) H. Huber, Thesis (University of Neuchâtel, Switzerland, 1974); H. Huber, C. Jaccard and M. Roulet, Rad. Eff. 12 (1972) 241; H. Huber, C. Jaccard and M. Roulet, *Physics and chemistry of ice*, Ottawa, 1972 (Royal Society of Canada, Ottawa, 1973) p. 137.
6) I. Golecki and C. Jaccard, to be published in J. Glaciology.
7) L. Meyer, Phys. Stat. Sol. (b) 44 (1971) 253.
8) A. Valenzuela and J. C. Eckardt, Rev. Sci. Instr. 42 (1971) 127., reported the preparation of a 7.6 nm silver foil.
9) J. S. Williams, Nucl. Instr. and Meth. 126 (1975) 205; E. Kasper and W. Pabst, Thin Solid Films 37 (1976) L5.
10) At higher pressures charge measurement is falsified by ionization of residual gas in the vicinity of the grid.
11) $dE/dx = 0.97$ keV/torr·cm for 100 keV protons in H_2O vapor at 0°C [3].
12)) Supersonic flow takes place because the ratio of the pressure in the HPC to that in the LSC exceeds 1.85, the critical ratio for H_2O vapor. See, e.g. L. D. Landau and E. M. Lifshitz, *Fluid mechanics* (Pergamon Press, London, 1959) ch. 9.
13)) This value agrees with the value of 0.67 $(keV)^2$/torr·cm reported for 95 keV protons in air by E. Bonderup and P. Hvelplund, Phys. Rev. A 4 (1971) 562.
14)) The Kodak CA-80-15 films were kindly provided by Dr. M. Monnin, University of Clermont-Ferrand, France. For applications see R. L. Fleischer, P. B. Price and R. M. Walker, *Nuclear tracks in solids* (University of California Press, Berkeley, 1975).
15)) I. Golecki and D. S. Tannhauser, J. Phys. E: Sci. Instr. 8 (1975) 21.

Accepted for publication in Proc. Symposium on the Physics and Chemistry of Ice, Cambridge, England, September 1977 : in J. Glaciology 21, No.85 (1978).

RADIATION DAMAGE IN ICE AT LOW TEMPERATURE STUDIED BY PROTON CHANNELING

I. GOLECKI* and C. JACCARD

Institut de Physique, Université de Neuchâtel
Rue A.-L. Breguet 1, CH-2000 Neuchâtel, Switzerland

*Present address: Electrical Engineering 116-81,
California Institute of Technology
Pasadena, CA 91125, USA.

ABSTRACT

100 keV protons with fluxes between 3×10^{15} and 3×10^{16} $m^{-2}s^{-1}$ and in doses up to 4×10^{20} m^{-2} have been used in ice between $-191^{o}C$ and $-87^{o}C$ to create damage and to analyze it. The Rutherford backscattering minimum yield along the c-axis (about 0.05 in good monocrystals) increases up to unity with the dose, according to a function which can be scaled by a critical dose depending mainly on temperature (Arrhenius law with activation enthalpy of 0.17 ± 0.04 eV above $-185^{o}C$). Higher flux produces more damage above $-180^{o}C$, but less below. A beam in a random direction is more efficient below $-180^{o}C$, but less at higher temperature than an aligned beam. Beam induced reordering is observed at definite temperatures and doses. The damage is shown to be due to energy loss by electronic excitations, which decay and produce disordered molecule clusters, mainly by incoherent aggregation of vacancies and interstitials.

RESUME

ETUDE PAR CANALISATION DE PROTONS DES DEGATS DE RADIATION DANS LA GLACE A BASSE TEMPERATURE

Des protons de 100 keV avec des flux compris entre 3×10^{15} et 3×10^{16} $m^{-2}s^{-1}$ et des doses jusqu'à 4×10^{20} m^{-2} ont été utilisés dans la glace entre $-191^{o}C$ et $-87^{o}C$ pour créer des dégâts et les analyser. Le rendement minimum de rétrodiffusion Rutherford le long de l'axe c (environ 0.05 dans de bons monocristaux) augmente jusqu'à l'unité avec la dose, selon une fonction faisant intervenir comme paramètre une dose critique dépendant surtout de la température (loi d'Arrhenius avec une enthalpie d'activation de 0.17 ± 0.04 eV en-dessus de $-185^{o}C$). Un flux plus élevé produit plus de dégâts en-dessus de $-180^{o}C$, mais moins en-dessous. Un faisceau dans une direction aléatoire est plus efficace en-dessous de $-180^{o}C$, mais l'est moins à des températures supérieures qu'un faisceau aligné. Une réordination induite par le faisceau est observée à des températures et doses bien définies. On montre que les dégâts sont dus aux pertes d'énergie par excitation électronique, donnant lieu à des domaines désordonnés produits surtout par l'agrégation de lacunes et d'interstitiels.

ZUSAMMENFASSUNG

UNTERSUCHUNG DURCH PROTONEN-CHANNELING VON STRAHLUNGSSCHADEN IN EIS BEI TIEFER TEMPERATUR

100 keV Protonen mit Flüssen zwischen 3×10^{15} und 3×10^{16} $m^{-2} s^{-1}$ und Dosen bis 4×10^{20} m^{-2} wurden in Eis zwischen $-191^{\circ}C$ und $-87^{\circ}C$ benützt, um Strahlungsschäden zu erzeugen and zu analysieren. Das minimale Rutherfurdsche Rückstreuvermögen entlang der c-Achse (etwa 0.05 in guten Einkristallen) nimmt mit der Dose zu (bis 1.0), und wird hauptsächlich von einer temperaturabhängigen, kritischen Dose bestimmt (Arrheniusgesetz mit 0.17 ± 0.04 eV Aktivierungsenthalpie oberhalb $-185^{\circ}C$). Ein höherer Fluss erzeugt mehr Schaden oberhalb $-160^{\circ}C$, aber weniger unterhalb dieser Temperatur. Ein zufällig gerichteter Strahl ist unter $-180^{\circ}C$ wirksamer als ein parallel zur c-Achse gerichteter Strahl, aber weniger bei höheren Temperaturen. Eine vom Strahl induzierte Unordnung wird bei wohl bestimmten Dosen und Temperaturen beobachtet. Die Schäden rühren von dem durch elektronische Anregungen verursachten Energie-Verlust her und bestehen aus ungeordneten Bezirken, welche hauptsächlich durch Agregation von Leerstellen und Zwischengittermolekülen entstehen.

1. INTRODUCTION

Since several decades, considerable interest has been devoted to radiation damage produced by energetic particles in solids, not only in view of technological applications (e.g. nuclear power) but also in order to assess the effect of nuclear technology or of outer space conditions on animate and inanimate matter. Although the damage mechanisms are complex, significant analogies can be found in quite different materials. We have been prompted to study the damaging effect of 100 keV protons in ice in the course of investigations by channeling of the surface structure of ice monocrystals (Huber et al., 1972, 1973; Huber, 1974). For details of the method, the reader is referred to a comprehensive review by Gemmell (1974). Briefly, one measures the backscattering yield, χ, by the crystal of a well-collimated proton beam. The yield is normalized to unity for the beam in a random direction, and it drops to a few percent when the beam is parallel to a principal crystallographic axis. Disorder, such as thermal vibrations, interstitials, or amorphous zones, shows up as an increase of the yield. The principal advantages of 100 keV protons versus higher energy protons in the case of ice are : 1) The stopping power has a flat maximum at 100 keV (Whaling, 1958), and thus the depth resolution is maximum too. 2) The stopping power is the same for an aligned and for a random beam, simplifying data evaluation. 3) The yield and "signal/damage" ratio are higher, since the Rutherford backscattering cross-section is inversely proportional to the energy squared.
In previous experiments, Huber (1974) found that the sensitivity to damage increased rapidly below $-150^{\circ}C$. At $-143^{\circ}C$, a dose of one proton per channel (parallel to the a-axis) increased the yield by less than 1%, whereas at $-170^{\circ}C$ one fifth of this dose brought the yield near unity, indicating complete loss of long-range order in the surface layer considered (240 nm). The temperature domain of this abrupt change coincides with other anomalies observed in the dielectric constant (Dengel et al., 1964), the protonic mobility (Eckener et al., 1973), the sound velocity (Helmreich and Bullemer, 1969), the specific heat (Matsuo et al., 1973) and even the scattering of γ-rays (Fitzgerald and O'Connor, 1976). The region is also critical

for the"amorphous-cubic" transition, and for vapour deposition on monocrystals : the deposited layer is coherent with the substrate only above -150°C (Huber, 1974). The possible relation of all these effects with the damage sensitivity, and the question of a beam-induced phase transition versus a thermally-activated process suggested a closer look at the damage formation in this temperature range. In this paper, we present some experimental details (section 2) and the results of the measurements (section 3). A tentative kinetic model, which is supported by the measurements, is discussed in section 4.

2. EXPERIMENTAL

The experimental apparatus, with the exception of several improvements, has been described in detail by Huber (1974). The 100 keV, 1 mm diameter proton beam is collimated by the ion optics to 0.05°. The scattering chamber is evacuated by means of a 350 l/s turbo-molecular pump (Leybold-Heraeus) to a hydrocarbon-free vacuum of 1×10^{-6} Torr. A 500 cm^2, LN_2-cooled copper trap serves to depress the partial pressure of water vapour to 2×10^{-9} Torr, equivalent to a dew point of -133°C. Thus the water-vapour condensation-rate on a sample maintained at -191°C is smaller than 3 monolayers/hour. The top flange of the scattering chamber accomodates a goniometer, on which is mounted a variable-temperature cryostat. The goniometer has four degrees of freedom : rotation (360°/ precision 0.05°), tilt (±10°/0.025°), vertical and horizontal translation (20 mm/0.01 mm and 12 mm/0.005 mm, respectively). The rotation and tilt axes cross one another at the surface of the sample. The cryostat which is cooled by LN_2 operates by gas exchange. The lowest achievable temperature is -191°C, and stable operation is possible up to room temperature.

The beam intensity is measured by intercepting part of it on a Micromesh nickel grid (EMI Electronics Ltd), of cell side 0.125 mm and 75% transmission. The positively biased grid, located at the entrance to the scattering chamber, is connected to a model 602 Keithley coulombmeter, the analog output of which

controls data acquisition. A second nickel grid, of cell side 0.013 mm and 30% transmission is placed on a mobile mount 20 mm in front of the insulating ice sample. Low-energy secondary electrons emitted by the negatively biased grid under proton irradiation serve to neutralize the positive charge carried by the proton beam to the surface of the sample. This grid has only negligible effect on beam divergence and energy profile; no sputtering of nickel atoms has ever been observed. The mobile mount also carries a pre-aligned, 0.28 mm diameter diaphragm which can be used to reduce the beam spot on the crystal. The backscattered protons are detected at 150° by means of a 25 mm^2 Si surface-barrier detector (Ortec premium) connected to standard spectroscopy electronics. The overall resolution with the detector cooled to 193 ± 5 K is 3 keV, corresponding to a depth resolution in ice of 16 nm. The system energy calibration is done by scattering off a thin target of Xe or Kr gas at 10^{-2} Torr, and can be checked with the aid of a 1 nm evaporated layer of Au on a Be substrate.

The pure, single crystal ice samples, typically 5 mm on a side, are cut on a refrigerated lathe from a larger oriented crystal (kindly provided by Dr. J.H. Bilgram, ETH, Zürich). The surface of the crystal is cleaned in situ prior to measurement by means of 3 keV Xe or Kr ion sputtering combined with sublimation at -80°C. The 2 mm diameter heavy-ion beam has an intensity of a few $\mu A/cm^2$. The proton irradiations are performed both along the c-axis (aligned direction) and 9° off the c-axis (random direction). Irradiations in the temperature range -191°C to -140°C have been carried out with fluxes of 3×10^{11} and 3×10^{12} $H^+/cm^2.s$ (low and high flux, respectively) up to a dose of 4×10^{16} H^+/cm^2 or 70 H^+/channel (this corresponds to 5×10^{11} rad). Some measurements have been extended to -87°C with a flux of 5×10^{13} $H^+/cm^2.s$ up to 150 H^+/channel (ca. 10^{12} rad). The crystal temperature is measured with a calibrated copper/constantan thermocouple.

The principal quantity measured as a function of dose is the minimum yield, χ, along the c-axis in a layer between 20 and 60 nm beneath the surface. In addition, backscattered energy spectra and angular scans are taken at various stages of the damage process. The known stopping power of protons in H_2O (Whaling, 1958), $dE/dx = 84.6 \pm 8$ eV/nm, is used to determine the energy-depth scale. Special care is needed for the measurement of the damage caused in random irradiations. In order to ensure that the minimum yield is measured exactly at the 1 mm diameter irradiated area, the surface of the crystal is scanned with a 0.28 mm diameter beam by shifting the cryostat assembly.

3. RESULTS

3.1 Aligned irradiations : $-191^{\circ}C \leq T \leq -140^{\circ}C$

The effect of radiation damage on the channeling dip (fig. 1) is mainly to increase the minimum yield above the undamaged value of about 0.05, the FWHM being only slightly reduced from 2.0° to 1.8°. At high dose, the channeling effect disappears altogether (i.e. $\chi = 1$), indicating either amorphization of the measured zone, or possibly a structure consisting of misaligned microcrystals. The exact nature of the defects can rarely be determined by channeling alone (see Quéré, 1976). In a typical sequence of backscattered energy spectra, the surface peak increases with dose, indicating the formation and progression of a disordered region from the surface of the crystal inwards. The aligned and random spectra eventually merge when long-range order has been lost.

Thevvariation of the damage curves $\chi(D)$ with temperature T and proton flux J is illustrated in fig. 2 for aligned irradiations. For fixed T and J, the minimum yield increases with dose, tending asymptotically to a saturation value of unity. On a linear dose scale, and at $T \leq -180^{\circ}C$, the curves have an exponential form (slope at the origin positive and maximum), while at higher temperatures they exhibit a sigmoid character, i.e. nearly zero slope at the origin, followed by an inflection point for

$\chi < 0.5$. An inflection point may exist even below $-180^{\circ}C$ at an immeasurably small dose. The temperature independence of the saturation value, as seen in particular in fig. 3 (discussed below), indicates that in the temperature range studied the irradiated region can always be amorphized completely. However, the measurements at $T \geq -156^{\circ}C$ were not taken to saturation, in order to avoid gross macroscopical damage effects*. The exact saturation value of χ depends on the choice of the random direction (Ziegler and Crowder, 1972), and therefore a 10% deviation about unity can be tolerated if the aligned spectrum has all the features of a random one. The dependence on the proton flux is such that at $T \geq -172^{\circ}C$ the high flux produces much more damage than the low flux, but near $-181^{\circ}C$ this dose-rate effect disappears, and is then even reversed at $-191^{\circ}C$. This behaviour led us to look for an annealing of the damage by monitoring the minimum yield as a function of time and temperature for crystal areas previously damaged to various levels. No purely thermal annealing could be observed for $T \leq -140^{\circ}C$ over a period of one day (at $T > -133^{\circ}C$ the crystal surface slowly evaporates, thus precluding any long term measurements). Therefore, any recovery effects must be attributed to the beam itself.

In an effort to identify common features of the damage curves, we observed that they could be superimposed on each other by merely shifting on the logarithmic dose scale, see fig. 3, thus suggesting the existence of a single relevant parameter $D_c = D_c(T,J)$. In fact, this picture is somewhat oversimplified, since the reduced representation actually results in a family of curves, which intersect at $\chi = 0.5$ because of the arbitrary definition of D_c. The nature of the temperature dependence of this characteristic dose D_c can be brought out by plotting $\log D_{1/2}$ or alternatively $\log (d\chi/dD)_{max}$, the maximum value of the slope, versus inverse temperature, as shown in fig. 4.

---

*E.g. blistering, bubble formation, radiation-induced stress, and sputtering. For the doses used in this study, separate measurements on ice films deposited on a Au on Be target showed sputtering to be entirely negligible.

In spite of some scattering in the experimental results, visual inspection indicates an Arrhenius plot to be appropriate for $T \gtrsim -182^{o}C$ ($\gtrsim -176^{o}C$) for low (high) flux irradiations, while at lower temperatures the T-dependence is clearly seen to weaken. The respective enthalpies, ΔH (low flux) = 0.16 ± 0.04 eV, ΔH (high flux) = 0.20 ± 0.05 eV, were obtained by least-squares fits, and verified to be significantly different by means of the usual statistical tests. The $D_{1/2}$ plots yielded the set of values ΔH (low flux) = 0.13 ± 0.04 eV and ΔH (high flux) = 0.21 ± 0.06 eV, which is statistically compatible with the previous set. These results, and especially the dose-rate dependence of ΔH, substantiat the existence of a radiation-assisted, thermally-activated annealir process alluded to above.

Two additional effects observed only when substantial damage had been done (i.e. for $\chi \gtrsim 0.5$) were (1) fluctuations in the minimum yield which were larger than expected from the statistics alone, and (2) a series of sudden drops in χ occurring at reproducible dose values, as seen in the curve at $-170^{o}C$ (low flux) in fig. 2 at 1 H^{+}/channel. A plot of log D_1, the dose at which the first drop occurred, versus inverse temperature yielded a straight line with an enthalpy of ΔH = 0.11 ± 0.03 eV, for both high and low flux, although the drops occurred at higher dose values in the former case. Similar effects have been reported for the alkali halides (Hollis, 1973), in $BaTiO_3$ (Gemmell and Mikkelson, 1972), and in Ge (Holmén and Högberg, 1972), but to our knowledge this is the first time that a thermally activated process has been shown to take place. In agreement with Hollis (1973), we believe that these effects are due to beam-induced rearrangement of displaced defects in the lattice. For instance, a clustering of interstitials may reduce χ by emptying some of the channels previously blocked by the same interstitials*.

* The hypothesis that non-neutralized positive charge in the bulk may be behind these effects was disproved by sub-surface potentia measurements of the ice crystal during irradiation with the aid of an electrostatic voltmeter.

3.2 Random irradiations : $-191^{o}C \leq T \leq -140^{o}C$

For the measurement of damage caused in random irradiations care had to be taken in order to avoid additional damage or annealing by the measuring beam. To this end, the following procedure was adopted : for each (T,J) set two series of irradiations were carried out with various doses at different but equivalent points on the crystal surface : one series in the random direction, and an identical one in the aligned direction. The minimum yield was then measured at $T \approx -155^{o}C$ with a small enough dose to avoid further damage. This method proved quite reliable through comparison with the known damage level in the aligned irradiations, but did not yield as detailed damage curves as for the latter. Nevertheless, the following conclusions were drawn : At $T \leq -180^{o}C$ random irradiation produced slightly more damage than aligned irradiation, but at higher temperatures this trend was reversed : at $T = -162^{o}C$ the damage caused by random irradiation was only half as large as that caused by aligned irradiation. This temperature dependence obtained for both low and high flux, thus indicating a dose-rate effect similar to that in aligned irradiations. No definite conclusion could be reached regarding the rearrangement effect because of the relatively small number of dose values per curve. Angular scans showed a similar shape as in aligned irradiations.

3.3 Aligned irradiations : $-130^{o}C \leq T \leq -87^{o}C$

In order to avoid sublimation of the surface during measurement, the crystal was kept in equilibrium with its own vapour in a special chamber (Golecki and Jaccard, to be published) fixed inside the large scattering chamber. The results obtained at $-130^{o}C$ were of the same nature as those previously described for lower temperatures. However, for $T \geq -115^{o}C$, a remarkable change in behaviour was observed to take place. The surface peak in the backscattered energy spectra disappeared with increasing dose, as the high-energy edge became rounded off. Furthermore, the sensitivity to radiation damage <u>increased</u> rapidly with temperature, in contradistinction to the observations

at $T \leqslant -130^{\circ}C$. The shape of the damage curves was sigmoid, and the rearrangement phenomenon was also observed in this temperature range. Initial analysis of the results yielded an activation enthalpy of about 0.4 eV. These observations indicate that a completely different damage mechanism operates in this temperature region, which includes the measurements previously reported by Huber et al. (1972). Probably the different behaviour should be attributed to different annealing and clustering properties of the defects in ice. A similar temperature dependence has been reported for silicon by Pabst and Palmer (1975).

4. DISCUSSION

The most conspicuous characteristic of the damage production is the occurrence of a "scaling law" with temperature as a parameter, intervening by means of the critical dose. According to phenomenological calculations, the heat conductivity suffices to evacuate the proton energy in such a way that the surface temperatu rise at the beam impact is smaller than $0.1^{\circ}C$. Thus the bulk temperature can be assumed to be relevant. The fact that the temperature dependenc$_e$ is continuous with an Arrhenius behaviour in a large range precludes any phase transition mechanism; it shows that near the surface, the local temperature is not influence significantly by the beam. There are certainly "thermal spikes", but the essential of the disorder producing mechanism happens quite near the bulk temperature, in a medium which is far from chemical equilibrium but nearly homogeneous.

The proton energy loss at the surface of 85 eV/nm is due mainly to electronic excitation. Elastic collisions with oxygen nuclei account for less than 1%, nevertheless, their efficiency to displace molecules has to be examined. An interstitial-vacancy pair requires at least 1 eV (to break 4 hydrogen bonds) and standard formulae (Nelson, 1968) give for 100 keV protons a cross-section of $\sigma_d = 5 \times 10^{-23}\ m^2$ for an energy transfer superior to this energy. If secondary collisions are taken into account, this value is

increased at most by a factor of ten, up to 5×10^{-22} m^2. If the dose D is expressed in proton per channel, with the channel area $F_c = 1.75 \times 10^{-19}$ m^2, the maximum relative concentration of interstitials amounts then to $c_i = D.\sigma_d/F_c \lesssim 3 \times 10^{-3} D$, which is nearly equal to the increase of the yield $\Delta\chi$ provided $\chi \ll 1$ and without thermal damage restoration, i.e. at low temperature. At $-180^{\circ}C$, the measurements give for the disorder growth rate $d\chi/dD = 4$ (proton/channel)$^{-1}$. The result of the calculation above lies three orders of magnitude lower, indicating that the observed disorder is not produced by direct nuclear collisions in ice. It has to be the result of the electronic excitation, which makes up almost the total energy loss.

The mechanism can be decomposed in three steps. First, the molecules are ionized, the electrons are shot into the conduction band where they excite secondary electrons, dispersing the energy around the trajectory of the incident proton. Hydrogen and OH bonds are ruptured, H and OH radicals are formed, as well as ions (OH^-, H_2O^+, etc.). All these species interact by numerous different reactions : The ions are neutralized rapidly by mobile electrons and holes, and the free radicals, which are mobile above $-180^{\circ}C$ (Eldrup, 1976), recombine also. The result of all these processes is, as a second step, the creation of several types of defects (vacancies, interstitial molecules, chemical compounds such as H_2, H_2O_2, etc.). Nuclear displacements happen either by multiple ionization process (Varley, 1962) or by de-excitation of trapped excitons (Itoh, 1976), a bimolecular species being violently separated in both cases and providing the necessary momentum. Since the vacancies are mobile above $-175^{\circ}C$ (Eldrup, 1976) with an activation enthalpy of 0.34 ± 0.07 eV, the defects should also be mobile in this temperature range.

In the present case, channeling is sensitive to oxygen nuclei displaced perpendicularly to the c-axis by at least their Thomas-Fermi radius (0.02 nm). Protons need not be considered; they are not detected at 150° backscattering and their cross-section for dechanneling is quite small. The temperature dependence of the damage formation suggests that the chemical reaction products (e.g. H_2O_2) are irrelevant for the following reasons. If they

are created during the thermal spikes, their formation is temperature independent, and if they are produced by a diffusive motion of the free radicals after the thermal spikes, their concentration should grow with the temperature. This disagrees with the observed decrease of the damage rate by increasing temperature. On the other hand, their production by the beam could be balanced by their diffusion towards the surface, giving the right temperature dependence. But then this diffusion should also occur without the beam, i.e. the damage should anneal, and this also contradicts the observations : once created, the damage does not anneal up to $-130^{\circ}C$. This last point, together with the fact that the relative concentration of the displaced oxygen atoms can be quite high (up to unity) if $\chi \sim 1$, can be accounted for by a damage consisting in clusters of molecules, either amorphous (below $-150^{\circ}C$) or crystallized, but not coherent with the original lattice. If they contain at-least 4-5 molecules, these clusters are stable with respect to thermal activation, e.g. interstitials or vacancies cannot "evaporate" from them.

The third step of the damage mechanism is then the formation of these clusters. A process generating them in a single shot and showing the correct temperature dependence is difficult to figure out. We rather suggest that they build up molecule after molecule. This can occur by successive aggregation of vacancies and interstitial H_2O molecules, which are produced in sufficient number near each proton trajectory and which diffuse freely after the thermal spike has dissipated, even at low temperature since their path is quite short. Then the temperature dependence of the critical dose does not reside in the diffusion but in the probability that each interstitial molecule trapped in a void on the surface of a cluster will bind with the cluster instead of binding in an ordered way with the surrounding lattice. This process is very improbable if the interstitial is trapped in a single vacancy, since it can be gripped there by its four bonds together and obliged to occupy a lattice site. But if it is trappe by a vacancy aggregate, it can be gripped only by one bond (or two) and it is quite possible that it takes a "wrong" place with respect to the lattice, especially when a second interstitial is also

trapped within a short time, binds the first one and stabilizes it. Vacancy aggregates have been postulated by Eldrup (1976), who mentions voids up to 1.5 nm diameter, and by Unwin and Muguruma (1972). Their creation can be explained by the attractive interaction between the vacancies, due to unsaturated H-bonds on the void surface. The elastic potential gives also an attraction between vacancies and interstitials, but a repulsion between interstitials. Therefore, the latter do not aggregate, but are trapped by vacancy clusters, which become filled up and thus cannot reach a very large size due to the high interstitial concentration.

The possibility of disordered agglomeration of interstitials in vacancy clusters is substantiated by the observation of Huber (1974) of noncoherent deposition of vapour on the crystal surface below $-150^{\circ}C$. Above this temperature, the domain structure is possibly cubic, but strongly distorted and anyway noncoherent with the matrix. At lower temperature, there is no experimental indication for order and the structure is certainly amorphous.

According to the measurements, the damage does not depend only on the properly reduced dose, but also on the proton flux. This implies that damage growth is not simply proportional to a reaction coefficient depending on temperature, but that it is the result of chain reactions between isolated vacancies, vacancy clusters, disordered domains and interstitials.

It is quite possible to write down a system of simultaneous differential equations describing the formation and the growth of the disordered domains, and involving the concentrations of all the filled and empty multivacancies. However, this introduces a large number of kinetic parameters (the reaction coefficients) which are unknown and cannot be determined from the measurements. Therefore, such a complicated calculation has no meaning in the present status of experiment, and we rather develop a semi-quantitative model. We assume that the concentration of the interstitials is stationary, i.e. those produced by the beam are continuously added to the disordered domains. If J is the flux (in $m^{-2}s^{-1}$) and k a coefficient for the defect yield (in m^{-1}), the beam creates then per unit time and in unit volume an amount of kJ defects. Since these have a meaning only in the ordered

lattice, we introduce the disordered volume fraction X, which can be equated in first approximation to the minimum yield χ. The average rate of interstitial production is therefore $kJ(1-X)$. In order to describe the time evolution of X, one has to introduce the probability P that an interstitial entering a disordered domain takes a "wrong" position with respect to the lattice. If v_o is the molecular volume (3×10^{-29} m^3) we have then

$$dX/dt = v_o kJ(1-X)P$$

or with the dose $D = Jt$

$$dX/dD = (1-X)v_o kP$$

From the measurements, we infer that P has the form

$$P = \frac{P_o}{1 + b\exp(-\Delta H/kT)}$$

ΔH could have the meaning of the potential step which has to be climbed over by a molecule to turn from a "wrong" to a "correct" position. At low temperature (-180°C), $P = P_o$; X grows as $1 - \exp(-D/D_c)$, with D_c independent of J and T. There is no inflection point. At higher temperature, P and D_c depend on T, and $0.13\ eV < \Delta H < 0.21\ eV$. At the beginning of the process ($D \ll D_c$), the small aggregates predominate, i.e. b is larger and P is smaller than at higher dose. This accounts for the presence of the inflection point.

The dependence on J can be explained in the following way. If J is large, the instantaneous interstitial concentration is large too and the time is short between the aggregation of an interstitial in a disordered domain and the aggregation of the next one. This increases the probability that the molecules are blocked in a "wrong" position.

The product kP_o can be evaluated from the measurements. At -180°C for $X \ll 1$, we have

$$dX/dD = 4\ (proton/channel)^{-1} = 7\times10^{-19}\ m^2$$

Then

$$kP_o = (dX/dD)/v_o = 2\times10^{10}\ m^{-1} = 20\ nm^{-1}$$

With inelastic losses of $S = 85\ eV/nm$, the energy E_o per displaced

oxygen atom is given by $E_o = S/k \approx P_o .4$ eV. Even if we assume that $P_o \approx 1$, the energy necessary to produce a Frenkel pair is larger than E_o because the number of displaced oxygen atoms is certainly larger than the number of clustered molecules : each cluster is surrounded by a strain field, and if the cluster size is not too large, the volume of the observable perturbed zone can be at least twice the cluster volume. One has anyhow to expect a Frenkel pair yield smaller than in other substances for the following reasons. Firstly, these measurements pertain to a highly perturbed lattice, the strength of which can be significantly reduced. Secondly, Frenkel pair formation does not imply electric charge separation as in ionic crystals, and the hydrogen bond is relatively weak. In covalently bonded crystals, such as silicon (Pabst and Palmer, 1975), sapphire, or quartz (Krefft et al., 1975), the damage results only from the elastic nuclear collisions, the sensitivity being reduced by 10^3 to 10^4 with respect to ice. Comparison with other physico-chemical studies (Eldrup, 1976; Buxton, 1977) is difficult because the radiation doses used in this work (between Gigarad to Terarad) are higher by several orders of magnitude and the crystal structure is severely perturbed.

5. CONCLUSION

The damage produced in ice 40 nm beneath the surface between -190^oC and -140^oC by high energy protons and consisting of displaced oxygen atoms can be revealed by means of proton channeling. This disorder is not the result of direct collisions but of a large number of fast chemical reactions initiated by the strong electronic excitation diffusing from the proton trajectories and leading to the homogeneous creation of point defects (vacancies, interstitials, H_2, H_2O_2, etc.). Their motion is thermally activated, and assisted at low temperature by the elastic deformation potential. They aggregate and build up domains disordered with respect to the lattice. Within these domains, the structure is certainly amorphous below -150^oC, and possibly cubic with short range order above this temperature. The probability that aggregated molecules are bound incoherently to the lattice is a decreasing function of temperature which appears in the behaviour of the critical dose. The disorder

cannot anneal in the considered temperature range. More informati could be obtained from experiments performed under other condition such as heavier projectiles (He^+), higher energies (some MeV), and by other surface investigation methods (LEED) which are sensitive to disorder.

ACKNOWLEDGMENTS

The participation of F. Rudolf at the early stages of this project is acknowledged. This work was supported by the Swiss National Science Foundation. It forms part of the Thesis to be submitted by I. Golecki to the Faculty of Sciences, University of Neuchâtel, in partial fulfilment of the requirements for the degree of Ph.D. in Physics.

REFERENCES

Buxton, GV et al (1977) "Two types of localized excess electron in crystalline D_2O ice". Canadian Journal of Chemistry, vol.55, no.7, p.2385-95.

Dearnaley, G (1975) "Atomic displacement mechanism in ion-bombarded semiconductors and insulators". Applied Physics Letters, vol.26, no.9, p.499-501.

Dengel et al (1964) "Ferroelectric behaviour of ice", by O. Dengel, U. Eckener, H. Plitz, and N. Riehl. Physics Letters, vol.9, p.291-2.

Eckener et al (1973) "Transit time measurement of protons in ice", by U. Eckener, D. Helmreich, and H. Engelhardt, in Physics and Chemistry of Ice, E. Whalley, S.J. Jones, and L.W. Gold, eds., Royal Society of Canada, Ottawa, p.242-5.

Eldrup, M (1976) "Vacancy migration and void formation in gamma-irradiated ice". Journal of Chemical Physics, vol.64, p.5283-90.

Fitzgerald, WJ and O'Connor, DA (1976) "Anomalies in the scattering of gamma-rays from single crystals of HF-doped ice-I_h around 100 K" Zeitschrift für Physik B, vol.24, p.1-5.

Gemmell, DS and Mikkelson, RC (1972) "Channeling of protons in thin $BaTiO_3$ crystals at temperatures above and below the ferroelectric Curie point". Physical Review B, vol.6, no.5, p.1613-35.

Gemmel, DS (1974) "Channeling and related effects in the motion of charged particles through solids" Review of Modern Physics, vol.46, no.1, p.129-227.

Golecki, I and Jaccard, C, to be published. "An apparatus for channeling experiments at Torr pressures" to be published in Nuclear Instruments and Methods.

Helmreich, D and Bullemer, B (1969) "Anormales elastisches Verhalten von Eis bei tiefen Temperaturen" Physics of Condensed Matter, vol.8, p.384-92.

Hollis, MJ (1973) "Channeling of 1 MeV He^+ ions in NaCl : Damage and temperature effects". Physical Review B, vol. 8, No.3, p.931-5.

Holmén, G and Högberg, P (1972) "A study of the production and removal of radiation defects in Ge using secondary electron emission". Radiation Effects, vol.12, p.77-85.

Huber et al (1972) "Surface structure of ice studied by proton channeling", by H. Huber, C. Jaccard, and M. Roulet. Radiation Effects, vol.12, p.241-5.

Huber et al (1973) "Channeling of H^+, D^+, and He^+ in ice : Surface disorder and chlorine location", by H. Huber, C. Jaccard, and M.Roulet, in Physics and Chemistry of Ice, E. Whalley, S.J. Jones, and L.W. Gold, eds., Royal Society of Canada, Ottawa, p.137-9.

Huber,H (1974) "Application de la canalisation de protons de 100 ke à l'étude de la structure superficielle de la glace à basse température". Ph.D. Thesis, Université de Neuchâtel.

Itoh, N (1976) "Formation of lattice defects by ionizing radiation in alkali halides". Journal de Physique, Colloque C7, suppl. au no. 12, tome 37, p.C7-27-45.

Krefft et al (1975) "Effect of ionizing radiation on displacement damage in ion-bombarded single crystal alpha-Al_2O_3 and alpha-SiO_2", by G.B. Krefft, W. Beezhold, and E.P. EerNisse, IEEE Transactions on Nuclear Science, vol. NS-22, No.6, p.2247-9.

Krefft, GB (1977)"Ionization-stimulated annealing effects on displacement damage in magnesium oxide". Journal of Vacuum Science and Technology, vol.14, No.1, p.533-6.

Matsuo et al (1973) "Relaxational proton ordering in two-dimensiona ices", by T. Matsuo, M. Oguni, O. Haida, H. Suga, and S. Seki, in Physics and Chemistry of Ice, E. Whalley, S.J. Jones, and L.W. Gold eds., Royal Society of Canada, Ottawa, p.272-7.

Nelson, RS (1968) "The observation of atomic collisions in solids" North-Holland Publishing Company, Amsterdam.

Quéré, Y (1976) "On 'measurements' of radiation damage by back-scattering experiments" Radiation Effects, vol.28, p.253-5.

Pabst, HJ and Palmer, DW (1975) "Indication for an ionization damag process in light ion irradiation damage in silicon", in Internation Conference on Atomic Collisions in Solids, Gatlinburg, Tenn., 1973, Plenum Press, New York, 1975, p.141-157.

Unwin, PNT and Muguruma, J (1972). "Electron microscope observation on the defect structure of ice", Physica Status Solidi, vol.14,p.20

Varley, HJO (1962) "Discussion of some mechanisms of F centre formation in alkali halides" Journal of Physics and Chemistry of Solids, vol.23, p.985-994.

Whaling, W (1958) "The energy loss of charged particles in matter", in Handbuch der Physik, S. Flügge, ed., vol. XXXIV, Springer, Berlin, 1958, p.193-217.

Ziegler,JF and Crowder, BL (1972) "Defining the 'random' spectrum as used in the channeling technique of nuclear backscattering", Applied Physics Letters, vol.20, No.4, p.178-9.

FIGURE CAPTIONS

Fig. 1 Angular dependence of the channeling yield along the c-axis in ice. The solid curve was measured on a freshly cleaned surface at $-140^{\circ}C$ (FWHM = $2\times1.0^{\circ}$). The dashed curve was measured at $-151^{\circ}C$ on an area previously irradiated with 0.8 H^+/channel in the random direction at $-182^{\circ}C$ (FWHM = $2\times0.9^{\circ}$). In both cases the scattering zone beneath the surface was 40 nm thick.

Fig. 2 Dose dependence of minimum yield in ice for aligned irradiations, measured in a 40 nm thick layer beneath the surface. 1 H^+/channel = 5.7×10^{14} H^+/cm^2.

Fig. 3 Reduced representation of the dose dependence of the minimum yield in ice, where $D_{1/2} = D(X=0.5)$. □: $-191^{\circ}C$, $J_>$; + : $-181^{\circ}C$, $J_<$; ○ : $-171^{\circ}C$, $J_>$; Z : $-171^{\circ}C$, $J_<$; S: $-162^{\circ}C$, $J_>$; ◇ : $-162^{\circ}C$, $J_<$; Y : $-150^{\circ}C$, $J_>$; X: $-140^{\circ}C$, $J_>$. $J_>$ and $J_<$ denote a proton flux of 3×10^{12} and 3×10^{11} $H^+/cm^2.s$, respectively. The curves have been smoothed for clarity.

Fig. 4 Temperature dependence of the maximum slope of the damage curves. Crosses refer to high proton flux, solid circles to low proton flux.

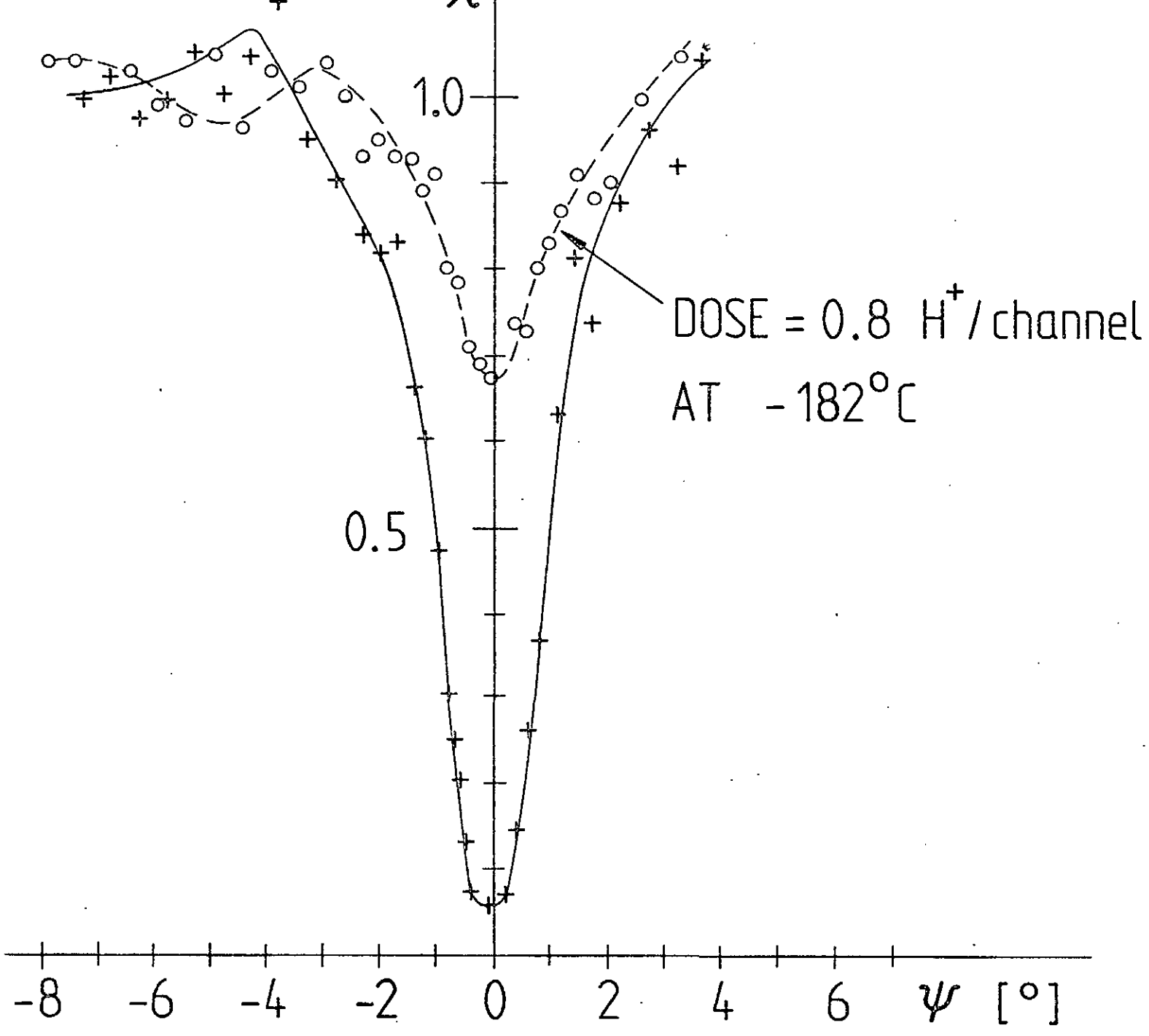
1.0
0.5
DOSE = 0.8 H+ / channel
AT -182°C
-8
-6
-4
-2
0
2
4
6
ψ [°]

Fig. 2

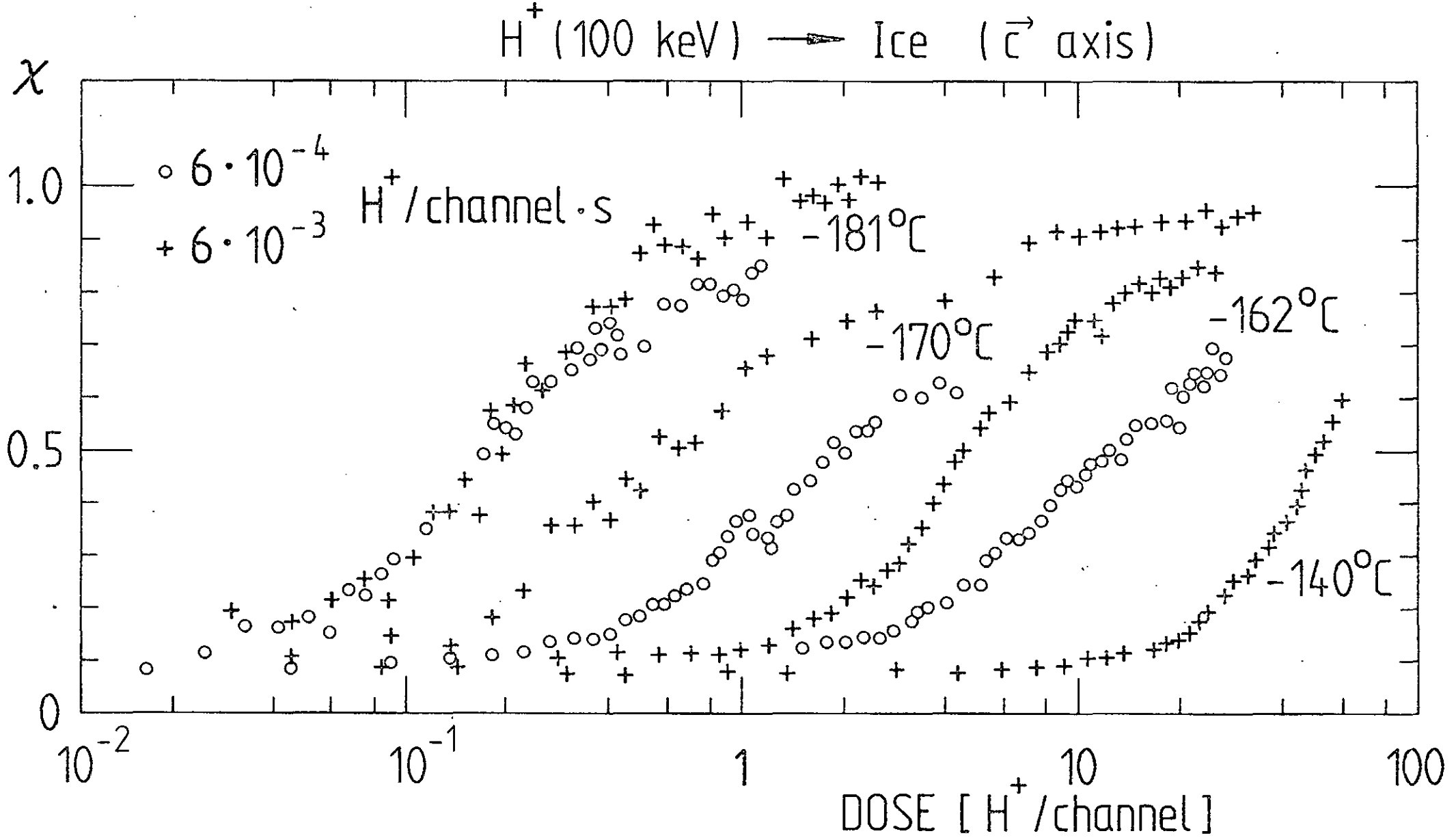
H+ (100 keV) → Ice (c axis)
χ
1.0
0.5
0
○ 6 · 10-4
+ 6 · 10-3
H+/channel · s
-181°C
-170°C
-162°C
-140°C
10-2
10-1
1
10
100
DOSE [H+/channel]

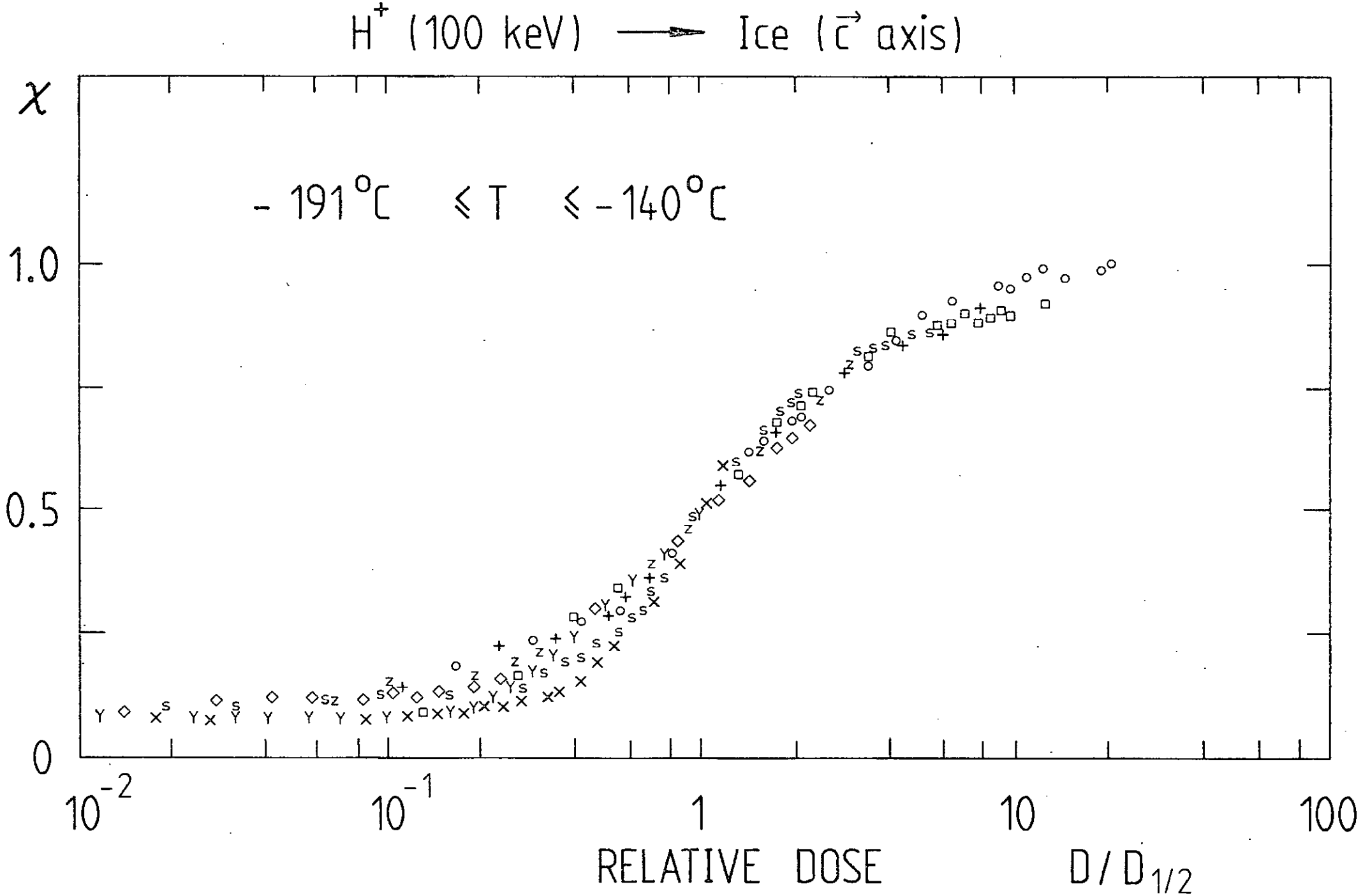
H+ (100 keV) ⟶ Ice (c⃗ axis)
χ
- 191°C ⩽ T ⩽ - 140°C
1.0
0.5
0
10-2
10-1
1
10
100
RELATIVE DOSE
D / D1/2

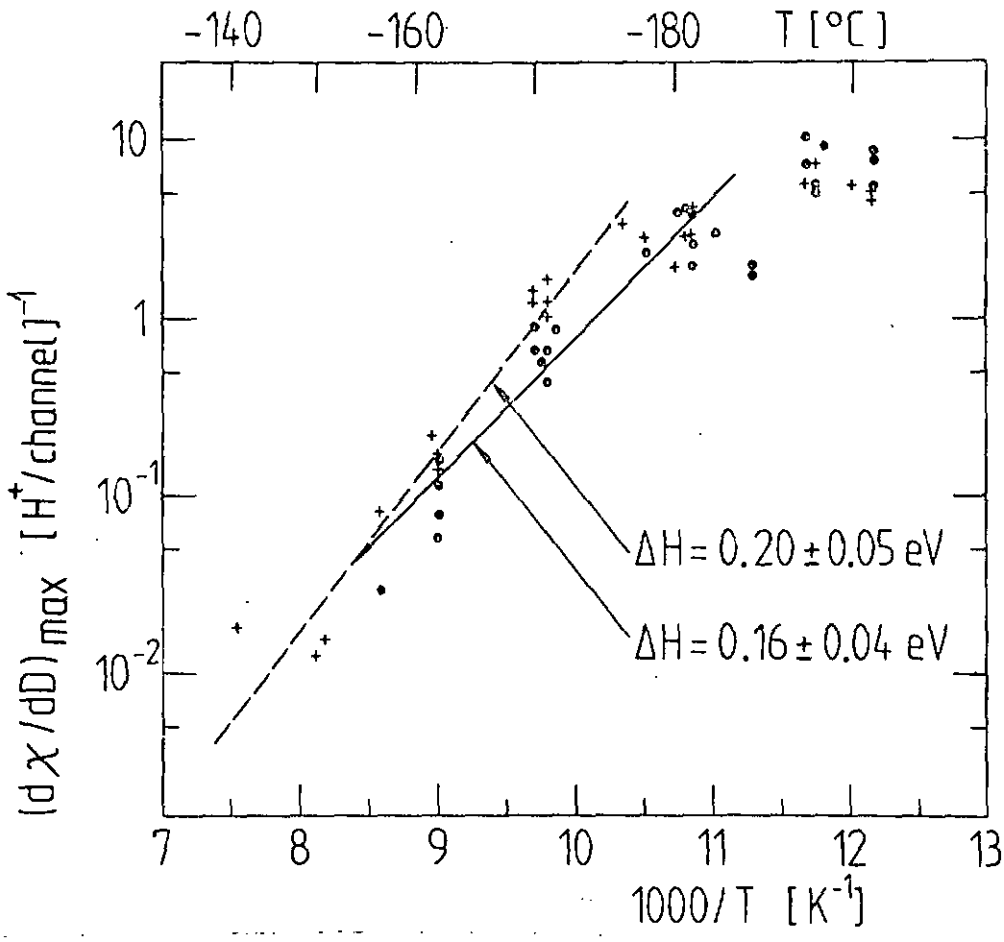
-140
-160
-180
T [°C]
10
1
10^{-1}
10^{-2}
$(d\chi/dD)_{max}$ [H+/channel]$^{-1}$
ΔH = 0.20 ± 0.05 eV
ΔH = 0.16 ± 0.04 eV
7
8
9
10
11
12
13
1000/T [K^{-1}]